CrossMark

ORIGINAL PAPER

Terpyridine functionalized α-cyanostilbene derivative as excellent fluorescence and naked eyes Fe²⁺ probe in aqueous environment

Xuan He[1] · Gao-Bin Zhang[1] · Zi-Xin Chi[1] · Peng-Fei Dai[1] · Jian-Yan Huang[1] ·
Jia-Xiang Yang[1]

Abstract A novel carbazole derivative (**L**) functionalized by terpyridine was designed and synthesized. Its structure was fully characterized by FT-IR, HR-MS, ¹H NMR spectra. **L** formed J-aggregates and possessed aggregation-induced emission enhancement property in aqueous environment. In addition, compound **L** showed specific response to Fe²⁺ in UV–vis spectra at 557 nm in EtOH–H₂O mixed solvent, owing to metal-to-ligand-charge-transfer (MLCT). The emission quenched much more sharply than other metal ions when adding Fe²⁺. The interaction between compound **L** and Fe²⁺ was analyzed by UV–vis and fluorescence spectrum titration. The limit of detection was calculated to be 1.63 μM. The stoichiometric of **L** and Fe²⁺ was 2:1 confirmed by Job's plots. Competition experiment indicated that other metal ions caused little interference. In this way, **L** could be a fluorescent and "naked eyes" probe for Fe²⁺ detection. This dual mode Fe²⁺ sensor can be considered to have potential value in practical applications.

Keywords Terpyridine · Carbazole derivative · Fe²⁺ · fluorescent probe

✉ Jia-Xiang Yang
jxyang@ahu.edu.cn

[1] College of Chemistry and Chemical Engineering, Anhui University, Hefei 230601, Anhui, People's Republic of China

Introduction

Iron is one of the essential trace elements in the human body, which plays an important role in many biological activities, including oxygen metabolism (Sundramoorthy et al. 2016; Kim et al. 2013), enzymatic catalysis (Nandhini et al. 2016), DNA synthesis (Wei et al. 2015). Both iron deficiency and overload can cause serious problems (Saleem and Lee. 2015; Zhu et al. 2015; Kim et al. 2016). Hypoferremia usually induces anemia and functional deficits, making people become susceptible to disease. Hyperferremia can cause cell/tissue damage and organ dysfunction. It has been reported that Alzheimer's disease is related to iron overload (Sahoo et al. 2012). Thus, developing efficient method to detect iron is imperative.

Up to now, the detection methods of iron ions include flow injection analysis (Elsuccary and Salem 2015), atomic absorption spectroscopy (Shamspur et al. 2005), cyclic voltammetry (Caprara et al. 2015), and chemosensors (Au-Yeung et al. 2013) et al. Compared with the instrumental analysis methods, time-consuming and high cost, chemosensors, especially fluorescent and the "naked eyes" colorimetric recognition methods are convenient, fast and cheap. However, numbers of fluorescent probes are non-emissive in aqueous solution for the aggregation-caused quenching (ACQ) effect which limited their practical applications. Aggregation-induced emission enhancement (AIEE) fluorophores are weak emission in dilute solutions and strongly emit in aggregation states, which open a way to design chemosensors to against ACQ (Mei et al. 2014, 2015). The α-cyanostilbene derivatives are representative AIEEgens (An et al. 2002). Based on our previous work, α-cyanostilbene unit functionalized with chelating group is an effective method for designing ions probes (Fang et al. 2016). Terpyridine group has strong

metal chelating ability and has unique advantages in the design of iron ions recognition probes (Ali et al. 2011; Brombosz et al. 2007). However, in the previous reports, most fluorophores detecting Fe^{2+} suffer from the interference of other metal ions, especially Fe^{3+}. Recently, a graphene oxide-terpyridine conjugate as a nano-chemosensor for Fe^{2+} in aqueous media was reported (Eftekhari-Sis and Mirdoraghi 2016), nevertheless, specific terpyridine functionalized Fe^{2+} probe was rare according to our investigation. Our group managed developing two kinds of terpyridine functionalized α-cyanostilbene derivatives which detected Fe^{2+} in aqueous environment (Liang et al. 2007; Zhang et al. 2014). Herein, we imagined to introduce carbazole unit, a famous fluorophores with high luminescence efficiency, hole-transporting moiety into the system to design a selective Fe^{2+} probe with AIEE properties.

In this work, a novel carbazole derivative with functionalized terpyridine (**L**) was synthesized. The photophysical properties of **L** were studied by UV–vis absorption spectroscopy and fluorescence spectroscopy. This sensitive probe exhibited excellent AIEE property and could be used to detect single Fe^{2+} in aqueous solution. Other metal ions including Fe^{3+} caused little interference. Fortunately, **L** could act as a dual mode Fe^{2+} sensor via UV–vis absorption spectroscopy and "naked eyes" recognition.

Experimental

All chemicals were commercially available and all solvents were purified by conventional methods before used. NMR spectra were recorded on a Bruker Avance 400 MHz spectrometer using $CDCl_3$ or DMF-d_7 as solvent. Chemical shifts were reported in parts per million (ppm) down field from TMS with the solvent resonance as the internal standard. Coupling constants (J) were reported in Hz and referred to apparent peak multiplications. Mass spectra were recorded on an Agilent 6410 LC–MS/MS system (USA) equipped with an electrospray ion source (ESI). UV–vis absorption spectra were recorded on a TU-1901 of Beijing Purkinje General Instrument Co., Ltd, spectrometer (slit: 5 nm, 3 nm) using samples in solutions. Fluorescence spectra were recorded with a RF-5301 PC fluorescence spectrometer. The stock solution (1×10^{-3} M) was prepared by dissolving probe **L** in DMF. For the UV–vis and fluorescence analysis, 50 μL of the stock solution of **L** in DMF was diluted to 5 mL DMF-H_2O mixture or EtOH-H_2O mixture (volume fraction of water accounts for 30%), respectively. Solutions of $MgSO_4$, $Al_2(SO_4)_3 \cdot 18H_2O$, $MnSO_4 \cdot H_2O$, $FeSO_4 \cdot 7H_2O$, $FeCl_3 \cdot 6H_2O$, $CoCl_2 \cdot 6H_2O$, $NiCl_2 \cdot 6H_2O$, $CuSO_4 \cdot 5H_2O$, $ZnSO_4 \cdot 7H_2O$, $AgNO_3$,

$CdSO_4 \cdot 8H_2O$, $BaCl_2 \cdot 2H_2O$, $Hg(ClO_4)_2 \cdot 3H_2O$, and $Pb(NO_3)_2$ were prepared by dissolving them in double distilled water. All samples were prepared at room temperature. The emission spectra were recorded when excited at 430 nm. All the measurements were carried out at room temperature.

The synthetic route of compound **L** was shown in Fig. 1. Compound **1** was prepared according to the literature methods (Jin et al. 2011; Constable and Ward. 1990; Potts and Konwar. 1991).

9-(4-Bromobutyl)-9*H*-carbazole (**2**): a mixture of carbazole (3.3 g, 20 mmol), 1,4-dibromobutane (20 mL), toluene (15 mL), and tetrabutylammonium bromide 1.0 g in 15 mL 50% aqueous sodium hydroxide solution were stirred at 45 °C for 3 h, and then cooled to RT. The mixture was stirred overnight. After extraction with CH_2Cl_2, the organic phase was washed by water and saturated salt water for three times, respectively, and dried with anhydrous sodium sulfate. The solvent was removed under reduced pressure. The crude product was recrystallized from ethanol to obtain a white powder (3.83 g, 66.3% yield).

9-(3-Bromopropyl)-9*H*-carbazole-3-carbaldehyde (**3**): 5.4 mL DMF (70 mmol), 6.4 mL (70 mmol) $POCl_3$ were cooled to 0 °C by an external ice bath. Later, compound **2** (7.0 g, 23.2 mmol) dissolved in 1,2-dichloroethane was added to the mixture. The mixture was stirred at 80 °C overnight, then, it was added to ice water. After neutralization to weak basicity by NaOH, the solution was extracted with CH_2Cl_2. The organic layer was dried over with anhydrous sodium sulfate and filtered. The solvent was removed under reduced pressure. The residue was purified by silica gel column chromatography (eluent: CH_2Cl_2) to afford a white solid (4.29 g, 56.1% yield). m. p. 83–85 °C; ^{1}H NMR ($CDCl_3$, 400 MHz) δ 1.828–1.898 (2H, m, CH_2), 2.067–2.140 (2H, m, CH_2), 3.532–3.563 (2H, t, $J = 6.0$ Hz, CH_2–O), 4.391–4.427 (2H, t, $J = 7.2$ Hz, CH_2–N), 7.331–7.367 (1H, t, $J = 7.2$ Hz, phenyl–H), 7.459–7.498 (2H, t, $J = 8.0$ Hz, phenyl–H), 7.537–7.575 (1H, t, $J = 7.6$ Hz, phenyl–H), 8.019–8.040 (1H, d, $J = 8.4$ Hz, phenyl–H), 8.164–8.184 (1H, d, $J = 8.0$ Hz, phenyl–H), 8.627 (1H, s, phenyl–H), 10.112 (1H, s, aldehyde–H); ^{13}C NMR ($CDCl_3$, 100 MHz): 26.356, 29.987, 42.676, 44.341, 108.826, 109.263, 120.506, 120.842, 123.066, 123.187, 123.949, 126.862, 127.312, 128.727, 141.044, 143.931, 191.688.

N-(2,2′:6,2″,-4- terpyridyl oxybutyl)-3-aldehyde carbazole (**4**): Compound **1** (145.0 mg, 484.5 μmol), compound **3** (160.0 mg, 484.5 μmol), and K_2CO_3 (80.4 mg, 581.7 μmol) were added in 4 mL acetonitrile and refluxed overnight. The hot mixture was filtrated. The residue was washed with acetonitrile and water. After using flash chromatography (eluent: CH_2Cl_2) to remove compound **3**,
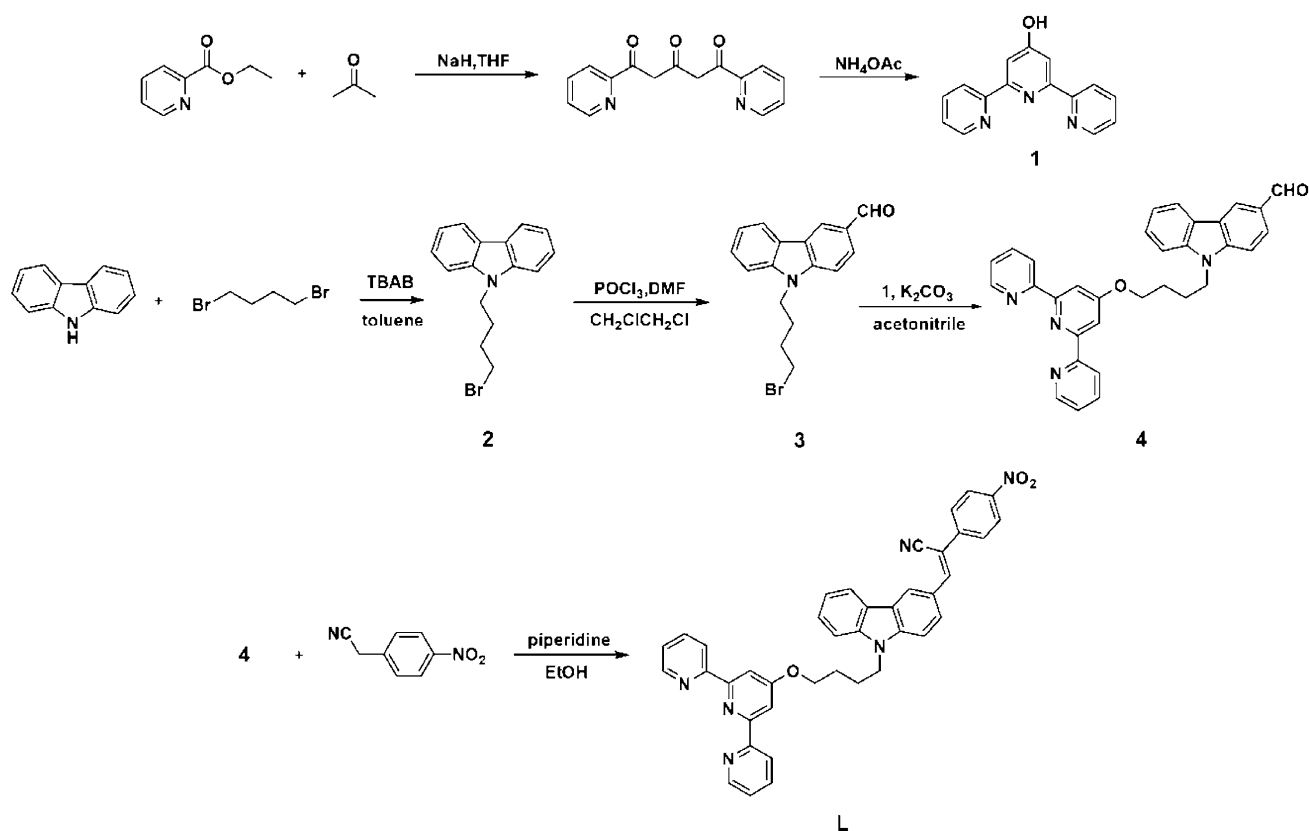
**Fig. 1** The synthetic route of compound **L**

the crude product was purified with chromatography (CH$_2$Cl$_2$/methanol = 10/1) to give a white solid product (118.0 mg, 48.9% yield). m.p. 180–181 °C; ^{1}H NMR (CDCl$_3$, 400 MHz), δ 1.909–1.976 (2H, t, J = 13.7, 7.3 Hz, CH$_2$), 2.129–2.202 (2H, m, CH$_2$), 4.240–4.269 (2H, t, J = 5.9 Hz, CH$_2$–N), 4.456–4.491 (2H, t, J = 7.1 Hz, CH$_2$–O), 7.304–7.355 (3H, m, phenyl–H), 7.485–7.564 (3H, m, phenyl–H), 7.839–7.881 (2H, m, phenyl–H), 7.987–8.030 (3H, m, phenyl–H), 8.141–8.160 (1H, d, J = 7.6 Hz, phenyl–H), 8.609–8.686 (5H, m, phenyl–H), 10.086 (1H, s, aldehyde–H); ^{13}C NMR (CDCl$_3$, 100 MHz,): 25.761, 26.700, 43.096, 67.581, 107.351, 108.944, 109.369, 120.427, 120.802, 121.411, 123.066, 123.192, 123.910, 126.863, 127.425, 128.653, 136.923, 141.118, 144.018, 148.954, 155.927, 157.061, 166.980, 191.748.

N-(2,2′:6,2″,-4-terpyridyl oxybutyl)-3-[2-(4-nitro-phenyl)-2-cyano]vinyl carbazole (*L*): Compound **4** (100.0 mg, 200 μmol), 2-(4-nitrophenyl)acetonitrile (39.0 mg, 240.5 μmol), 2 mL tetrahydrofuran and a drop of piperidine were added into 4 mL ethanol. The mixture was refluxed for 8 h and filtered. The residue was recrystallized from ethanol as an orange powder (50.0 mg, 38.8% yield). m.p. 261–263 °C; ^{1}H NMR (DMF-d_7, 400 MHz), δ 2.225 (2H, s, CH$_2$), 2.395 (2H, s, CH$_2$), 4.562–4.591 (2H, t,

J = 5.8 Hz, CH$_2$–N), 4.906–4.941 (2H, t, J = 6.9 Hz, CH$_2$–O), 7.517–7.554 (1H, t, J = 7.4 Hz, phenyl–H), 7.681–7.712 (2H, m, phenyl–H), 7.762–7.803 (1H, d, J = 8.0 Hz, phenyl–H), 8.051–8.071 (2H, d, J = 7.9 Hz, phenyl–H), 8.176 (2H, s, phenyl–H), 8.337–8.359 (1H, d, J = 8.7 Hz, phenyl–H), 8.405–8.424 (2H, t, J = 8.3 Hz, phenyl–H), 8.542–8.584 (2H, m, phenyl–H), 8.617–8.640 (2H, d, J = 9.1 Hz, phenyl–H), 8.707 (1H, s, phenyl–H), 8.877–8.929 (4H, m, phenyl–H), 9.134 (1H, s, CH); HR-MS (ESI–MS): m/z = 643.2466, calcd for [C$_{40}$H$_{31}$N$_6$O$_3$]$^+$ = 644.2458 ([M+H]$^+$).

Results and discussion

Water is a poor solvent and DMF is a good solvent for compound **L**. In DMF-H$_2$O mixed solvent, with the increase of water fraction (f_w), UV–vis absorption spectra showed broadened absorption accompanying with a red-shift (Fig. 2a). The light scattering tails were the characteristic of Mie effect, suggesting that compounds formed J-aggregate (Liang et al. 2016). In Fig. 2b, the peak at 425 nm in the transmittance spectra became weak when f_w changed from 10 to 30 vol%. Later the transmittance started to decrease while water continually added. The peak reappeared when f_w
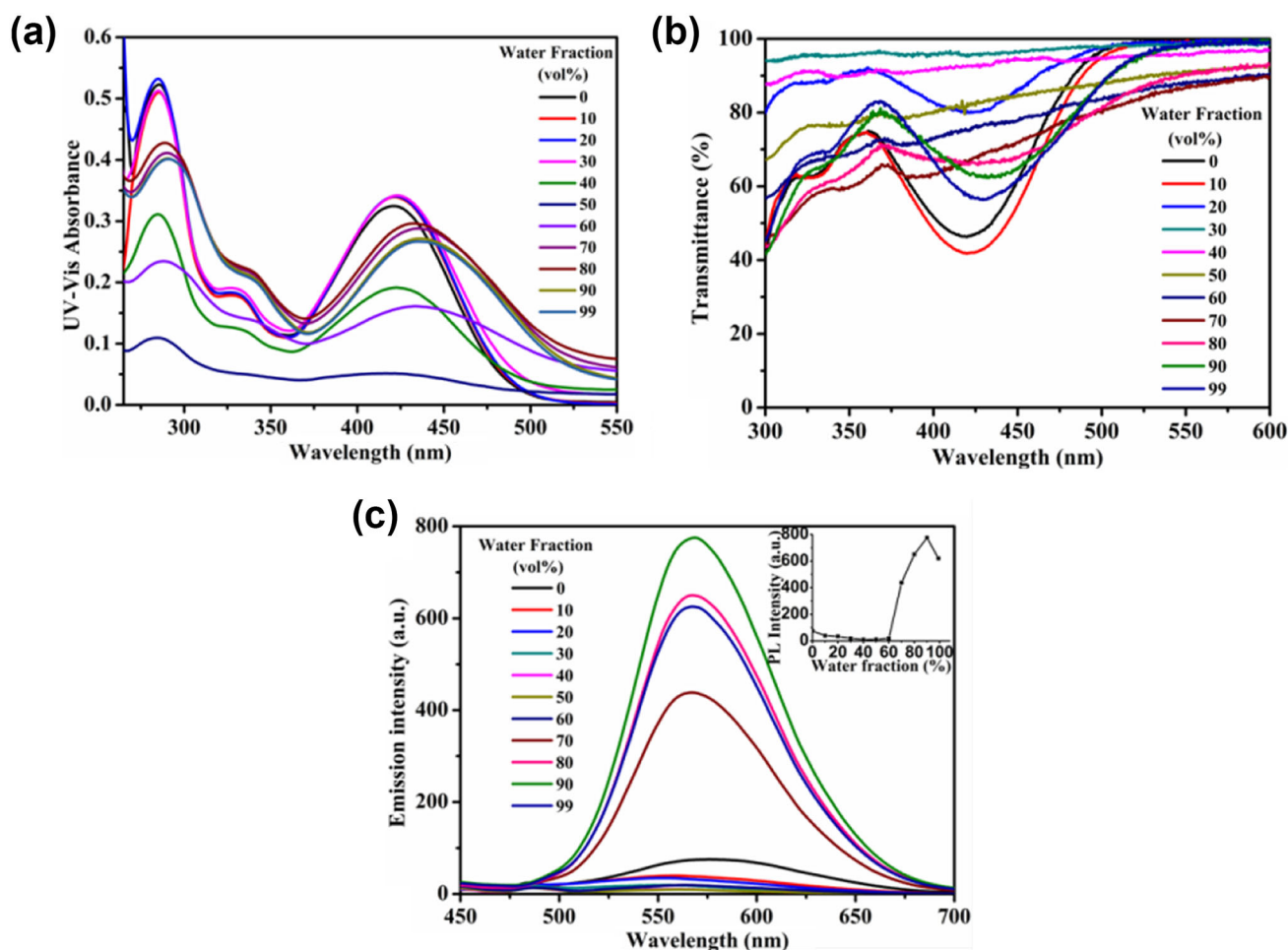
Fig. 2 UV–vis (**a**) and transmittance (**b**) and emission (**c**) spectra of compound **L** (10 μM) in DMF–H$_2$O mixture with volume fractions. *Insets* relation between fluorescence maximum intensity of compound **L** and volume fraction of water

was above 80 vol%, which was consistent with the absorption peak in UV–vis absorption spectra. In Fig. 2c, compound **L** had faint emission in pure DMF solution. With an increasing content of water from 0 to 60 vol%, the emission decreased swiftly. The decreased solubility of compound **L** in the aqueous mixture with high water content induced aggregate formation, which boosted the fluorescence emission. After f_w was above 90 vol%, the emission intensity of compound **L** began to decrease slightly. It is remarkable that the formation of J-aggregate expanded the area of π-conjugation, which was also in favor of the enhancement of emission. All of the above indicated that compound **L** exhibited obvious AIEE property.

To evaluate the recognition ability of compound **L** to metal ions, the UV–vis absorption spectra and emission spectra of **L** in the same concentration of metal ions were determined. As shown in Fig. 3, the solution with Fe^{2+} turned to brick red, while some other solutions such as solution with Mg^{2+} or Pb^{2+} exhibited a negligible light green color. The main reason was a characteristic peak formed in

UV–vis absorption spectra at 557 nm when Fe^{2+} was added (Fig. 4a). This phenomenon was attributed to metal-to-ligand-charge-transfer (MLCT) (Meier and Schubert. 2005). To identify Fe^{2+} state after FeSO$_4$·7H$_2$O was added into **L** in EtOH, the mixture was evaporated in vacuum. The XPS experiment results verified there were Fe^{2+} existed in the mixture (Fig. S6). It was indicated that compound **L** had specific colorimetric recognition towards Fe^{2+}, which could be used as a method of fast "naked eyes" detection. Moreover, after adding Fe^{2+}, the emission quenched much more sharply than that of other metal ions (Fig. 4b). Therefore, compound **L** could also become a fluorescent probe for Fe^{2+}. More evidence is shown in Fig. 5. After adding Fe^{2+}, the absorbance at 557 nm of **L** was three times more than other metal ions, indicating that other metal cations caused little interference in absorbance.

To investigate the interaction between compound **L** and Fe^{2+}, a titration experiment was studied. The concentration of **L** was 1.0×10^{-5} M. As shown in Fig. 6a, with the increase of Fe^{2+} concentration, a new peak at 557 nm in

Fig. 3 Color change of compound **L** (10 μM) in the presence of metal ions in EtOH–H$_2$O mixed solvent
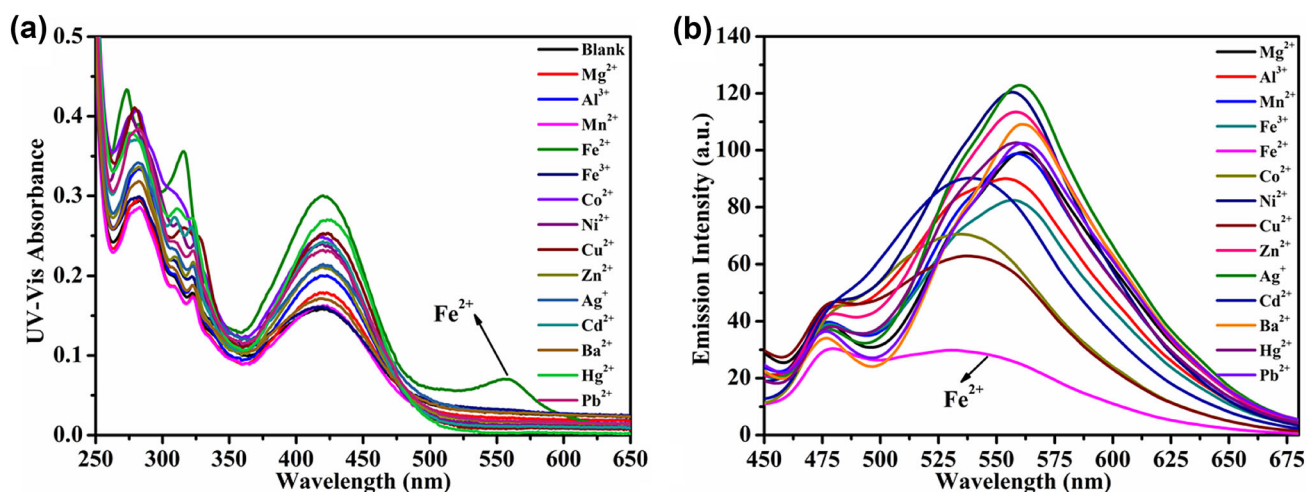
Fig. 4 UV–vis (**a**) and emission (**b**) spectra of compound **L** (10 μM) in EtOH–H$_2$O mixture (volume fraction of water accounts for 30%) after adding equivalent of various metal ions
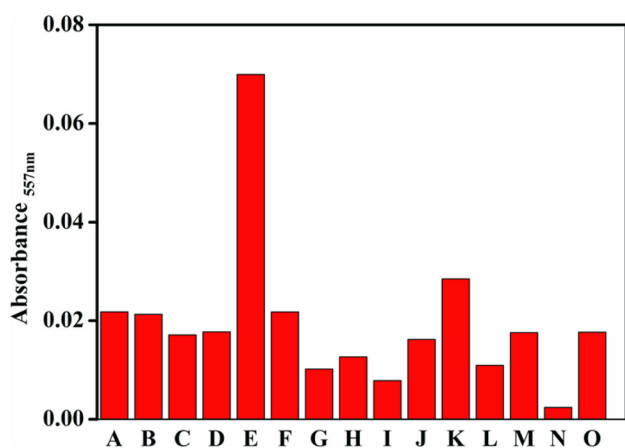
Fig. 5 Absorbance at 557 nm of compound **L** (10 μM) in EtOH–H$_2$O mixed solvent after adding equivalent of various metal ion. X-axis: *A* blank, *B* Mg^{2+}, *C* Al^{3+}, *D* Mn^{2+}, *E* Fe^{2+}, *F* Fe^{3+}, *G* Co^{2+}, *H* Ni^{2+}, *I* Cu^{2+}, *J* Zn^{2+}, *K* Ag$^+$, *L* Cd^{2+}, *M* Ba^{2+}, *N* Hg^{2+}, and *O* Pb^{2+}

UV–vis absorption spectra was observed. The absorbance began increasing linearly with the titration of Fe^{2+} then it reached a maximum as soon as Fe^{2+} was 5 μM. A binding 2:1 stoichiometry (**L**: Fe^{2+}) was further verified by Job's plot (Fig. 7). In order to test the sensitivity of Fe^{2+}, we studied fluorescent titration as shown in Fig. 6b. When the concentration of Fe^{2+} varied from 0 to 5 μM, the emission was weaken obviously, accompany with the peak at 560 nm blue-shifted by 30 nm. Then it changed very slowly. The limit of detection was calculated as low as 1.63 μM. The formula used was: DL = $3\delta/S$, where δ is the standard deviation of blank measurement, S is the slope between the ratio of absorbance versus respective analyte concentration.

The binding behavior of **L** towards Fe^{2+} ions and other competitive metal cations was investigated. The black bars represented the absorbance of one equivalent of **L** mixed with one equivalent of other metal ions and Fe^{2+} ions. As shown in Fig. 8, except for Co^{2+} and Cu^{2+}, no significant interference was observed, indicating that **L** could detect Fe^{2+} in presence of other metal ions.

Conclusions

In conclusion, we designed and synthesized a novel ter-pyridine modified carbazole derivative **L**, which had excellent AIEE property in aqueous environment. This
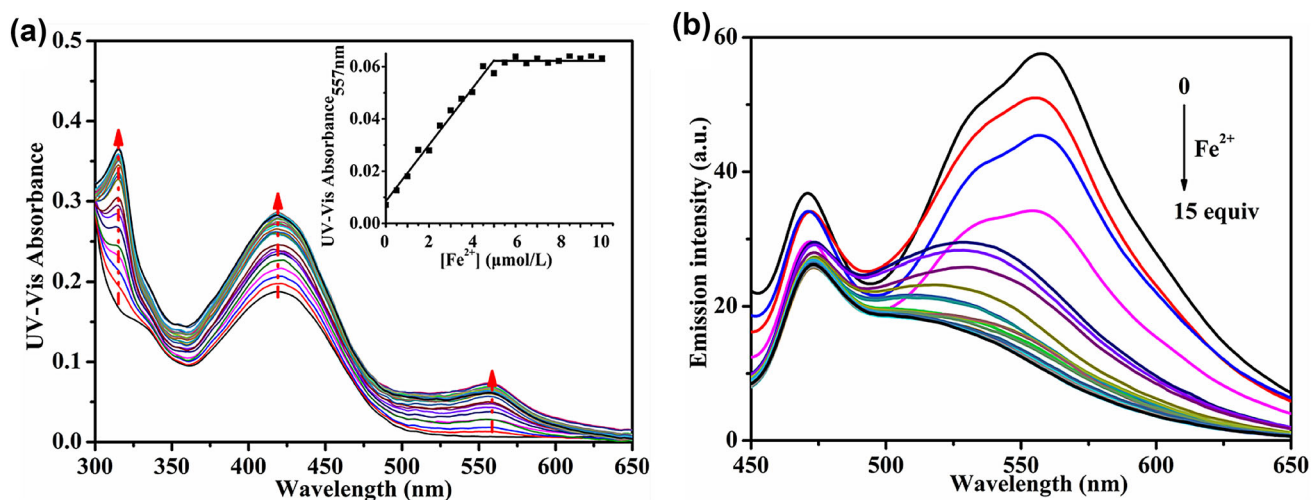
Fig. 6 UV–vis (**a**) and emission (**b**) spectra of compound **L** (10 μM) in EtOH–H$_2$O mixture (volume fraction of water accounts for 30%). *Insets* relation between absorbance of compound **L** at 557 nm and concentrations of Fe^{2+}
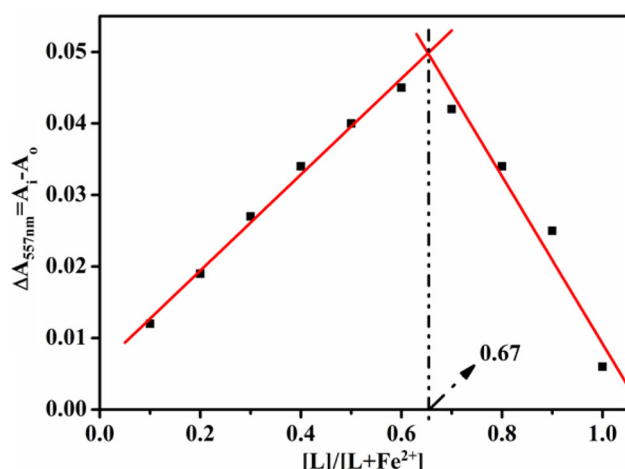
Fig. 7 Job's plot curve of **L** with Fe^{2+} ions
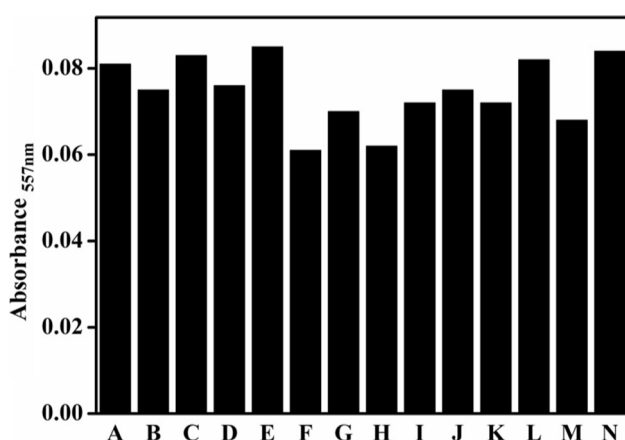
Fig. 8 *Bars* represent competitive selectivity of **L** (10 μM) in solvent mixture of EtOH–H$_2$O (volume fraction of water accounts for 30%) toward Fe^{2+} cation. *X*-axis: *A* Fe^{2+}, *B* Mg^{2+}+Fe^{2+}, *C* Al^{3+}+Fe^{2+}, *D* Mn^{2+}+Fe^{2+}, *E* Fe^{3+}+Fe^{2+}, *F* Co^{2+}+Fe^{2+}, *G* Ni^{2+}+Fe^{2+}, *H* Cu^{2+}+Fe^{2+}, *I* Zn^{2+}+Fe^{2+}, *J* Ag$^+$+Fe^{2+}, *K* Cd^{2+}+Fe^{2+}, *L* Ba^{2+}+Fe^{2+}, *M* Hg^{2+}+Fe^{2+}, and *N* Pb^{2+}+Fe^{2+}

probe could specifically detect Fe^{2+} by "naked eyes" colorimetric recognition and fluorescent recognition in the mixed solvent of EtOH–H$_2$O ($f_w = 30\%$), with high sensitivity. The limit of detection was determined to be 1.63 μM. We believed that functionalized terpyridine with α-cyanostilbene could be extended as a guide for the further design of AIEE probes detecting transition metal ions.

References

Ali M, Nasir S, Nguyen QH, Sahoo JK, Tahir MN, Tremel W, Ensinger W (2011) Metal ion affinity-based biomolecular recognition and conjugation inside synthetic polymer nanopores modified with iron-terpyridine complexes. J Am Chem Soc 133:17307–17314. doi:10.1021/ja205042t

An BK, Kwon SK, Jung SD, Park SY (2002) Enhanced emission and its switching in fluorescent organic nanoparticles. J Am Chem Soc 124:14410–14415. doi:10.1021/ja0269082

Au-Yeung HY, Chan J, Chantarojsiri T, Chang CJ (2013) Molecular imaging of labile iron(II) pools in living cells with a turn-on fluorescent probe. J Am Chem Soc 135:15165–15173. doi:10.1021/ja4072964

Brombosz SM, Zucchero AJ, Phillips RL, Vazquez D, Wilson A, Bunz UHF (2007) Terpyridine-based cruciform-Zn^{2+} complexes as anion-responsive fluorophores. Org Lett 9:4519–4522. doi:10.1021/ol7020302

Caprara S, Laglera LM, Monticelli D (2015) Ultrasensitive and fast voltammetric determination of iron in seawater by atmospheric oxygen catalysis in 500 μL samples. Anal Chem 87:6357–6363. doi:10.1021/acs.analchem.5b01239

Constable EC, Ward MD (1990) Synthesis and co-ordination behaviour of 6',6''-bis(2-pyridyl)-2,2': 4,4'':2'',2'''-quaterpyridine; 'back-to-back' 2,2': 6',2''-terpyridine. J Chem Soc Dalton Trans 4:1405–1409

Eftekhari-Sis B, Mirdoraghi S (2016) Graphene oxide-terpyridine conjugate: a highly selective colorimetric and sensitive fluorescence nano-chemosensor for Fe^{2+} in aqueous media. Nanochem Res 2:214–221. doi:10.7508/ncr.2016.02.008

Elsuccary SAA, Salem AA (2015) Novel flow injection analysis methods for the determination of total iron in blood serum and water. Talanta 131:108–115. doi:10.1016/j.talanta.2014.07.068

Fang WY, Zhang GB, Chen J, Kong L, Yang LM, Bi H, Yang JX (2016) An AIE active probe for specific sensing of Hg^{2+} based on linear conjugated bis-Schiff base. Sens Actuators B 229:338–346. doi:10.1016/j.snb.2016.01.130

Jin H, Zhang W, Wang D, Chu ZZ, Shen ZH, Zou DC, Fan XH, Zhou QF (2011) Dendron-jacketed electrophosphorescent copolymers: improved efficiency and tunable emission color by partial energy transfer. Macromolecules 44:9556–9564. doi:10.1021/ma2018556

Kim KB, Kim H, Song EJ, Kim S, Noh I, Kim C (2013) A cap-type Schiff base acting as a fluorescence sensor for zinc(II) and a colorimetric sensor for iron(II), copper(II), and zinc(II) in aqueous media. Dalton Trans 42:16569–16577. doi:10.1039/c3dt51916c

Kim H, Rao BA, Jeong J, Angupillai S, Joon JS, Nam JO, Lee CS, Son YA (2016) A rhodamine scaffold immobilized onto mesoporous silica as a fluorescent probe for the detection of Fe(III) and applications in bio-imaging and microfluidic chips. Sens Actuators B 224:404–412. doi:10.1016/j.snb.2015.10.058

Liang ZQ, Wang CX, Yang JX, Cao HW, Tian YP, Tao XT, Jiang MH (2007) A highly selective colorimetric chemosensor for detecting the respective amounts of iron(II) and iron(III) ions in water. New J Chem 31:906–910. doi:10.1039/b701201m

Liang KC, Dong LC, Jin N, Chen DD, Feng X, Shi JB, Zhi JG, Tong B, Dong YP (2016) The synthesis of chiral triphenylpyrrole derivatives and their aggregation-induced emission enhancement, aggregation-induced circular dichroism and helical self-assembly. RSC Adv 6:23420–23427. doi:10.1039/c5ra26985g

Mei J, Hong YN, Lam JWY, Qin AJ, Tang YH, Tang BZ (2014) Aggregation-induced emission: the whole is more brilliant than the parts. Adv Mater 26:5429–5479. doi:10.1002/adma.201401356

Mei J, Leung NLC, Kwok RTK, Lam JWY, Tang BZ (2015) Aggregation-induced emission: together we shine, united we soar! Chem Rev 115:11718–11940. doi:10.1021/acs.chemrev.5b00263

Meier MAR, Schubert US (2005) Fluorescent sensing of transition metal ions based on the encapsulation of dithranol in a polymeric core shell architecture. Chem Commun 36:4610–4612. doi:10.1039/b505409e

Nandhini T, Kaleeswaran P, Pitchumani K (2016) A highly selective, sensitive and "turn-on" fluorescent sensor for the paramagnetic Fe^{3+} ion. Sens Actuators B 230:199–205. doi:10.1016/j.snb.2016.02.054

Potts KT, Konwar D (1991) Synthesis of 4′-vinyl-2,2′: 6′,2″-terpyridine. J Org Chem 56:4815–4816

Sahoo SK, Sharma D, Bera RK, Crisponi G, Callan JF (2012) Iron(III) selective molecular and supramolecular fluorescent probes. Chem Soc Rev 41:7195–7227. doi:10.1039/c2cs35152h

Saleem M, Lee KH (2015) Optical sensor: a promising strategy for environmental and biomedical monitoring of ionic species. RSC Adv 5:72150–72287. doi:10.1039/c5ra11388a

Shamspur T, Sheikhshoaie I, Mashhadizadeh MH (2005) Flame atomic absorption spectroscopy (FAAS) determination of iron(III) after preconcentration on to modified analcime zeolite with 5-((4-nitrophenylazo)-N-(2′,4′-dimethoxyphenyl))salicylaldimine by column method. J Anal At Spectrom 20:476–478. doi:10.1039/b416097e

Sundramoorthy AK, Premkumar BS, Gunasekaran S (2016) Reduced graphene oxide-poly(3,4-ethylenedioxythiophene) polystyrene-sulfonate based dual-selective sensor for iron in different oxidation states. ACS Sens 1:151–157. doi:10.1021/acssensors.5b00172

Wei PF, Li DB, Shi BB, Wang Q, Huang FH (2015) An anthracene-appended 2:3 copillar[5]arene: synthesis, computational studies, and application in highly selective fluorescence sensing for Fe(III) ions. Chem Commun 51:15169–15172. doi:10.1039/c5cc06682d

Zhang GB, Liu J, Pan Y, Zhang RL, Kong L, Huang JY, Yang JX (2014) Synthesis of a terpyridine derivative for detection of Fe^{2+}. Chin J Inorg Chem 30:2699–2705. doi:10.11862/CJIC.2014.369

Zhu H, Fan JL, Wang BH, Peng XJ (2015) Fluorescent, MRI, and colorimetric chemical sensors for the first-row d-block metal ions. Chem Soc Rev 44:4337–4366. doi:10.1039/c4cs00285g